Biosensors and Bioelectronics 124–125 (2019) 224–232

Contents lists available at ScienceDirect

Biosensors and Bioelectronics

journal homepage: www.elsevier.com/locate/bios

A signal amplification system constructed by bi-enzymes and bi-nanospheres for sensitive detection of norepinephrine and miRNA

Tao Chen[a,1], Yuanhong Xu[b,*,1], Shuang Wei[a], Aihua Li[a], Lei Huang[b], Jingquan Liu[a,b,**]

[a] College of Materials Science and Engineering, Institute for Graphene Applied Technology Innovation, Collaborative Innovation Centre for Marine Biomass Fibers, Materials and Textiles of Shandong Province, Qingdao University, Qingdao 266071, China
[b] College of Life Sciences, Qingdao University, Qingdao 266071, China

ARTICLE INFO

Keywords:
Bi-enzymes
Bi-nanospheres
Signal amplification
Norepinephrine
MiRNA

ABSTRACT

Achieving the enhanced sensitivity and stability is always the pursuit for the fabrication of enzymatic biosensors. However, their sensitivity was still restricted by the fluctuant detection target (e.g. concentration), complex detection environment and limited recognition capability of enzymes. Herein, an effective and facile approach was designed to construct a bi-enzymatic and bi-nanospherical signal amplification system for fabrication of biosensors based on the designed polydopamine(PDA)-laccase@Au-glucose dehydrogenase. Therein, laccase-catalytic polymerized PDA nanoparticles (NPs) provided the supporting matrix for immobilization of laccase and AuNPs. The AuNPs with good conductivity and large surface area were used not only as a platform for enhanced loading capacity of glucose dehydrogenase but also as a conducting medium for electron transfer acceleration between enzymes and electrode. Moreover, the coordinated catalysis of bi-enzymes (laccase and glucose dehydrogenase) could avoid the fluctuated concentration of detection target (e.g. norepinephrine), while the application of bi-nanospheres loaded with large amount of enzymes could effectively amplify the signal of biosensors. Taking advantages of these merits, the as-prepared biosensors showed preeminent reproducibility, larger detection range from 0.5 nM to 0.5 μM, and lower detection limit of 0.07 nM (S/N = 3) for the norepinephrine detection. Besides, the constructed PDA-laccase@Au-glucose dehydrogenase was also successfully applied as the sensing probes for the detection of microRNA (miRNA), especially for single-nucleotide mismatched miRNA via specific recognition.

1. Introduction

Electrochemical biosensors, which contain the biological recognition element (e.g. enzymes, antibodies, receptors, proteins, nucleic acids, tissues or cells) that could selectively react with the targeted analyte and produce a related electrical signal, have drawn increasing attention due to their obvious advantages such as high specificity, fast analyzing speed and reusability (Chen et al., 2013, 2017; He et al., 2015; Li et al., 1996; Rasooly and Herold, 2006; Song et al., 2016). Thereinto, the study of enzymatic biosensors (Sassolas et al., 2012; Zhang et al., 2010) has gone through a fast development period, plentiful of biosensors with various functions based on different enzymes such as glucose oxidase (Wooten et al., 2014), horseradish peroxidase (Lu et al., 2006; Zhang et al., 2008), laccase (Chen et al., 2017), protease (Qiao et al., 2015), lipase (Chao et al., 2014), have been fabricated and applied in various fields. However, in the biosensing process, enzymes usually react with the targeted analyte, resulting in nonnegligible influence on the detection sensitivity, especially in the detection of analyte at very low concentrations (Kwok et al., 2015; Lanzellotto et al., 2014; Shen et al., 2014). Therefore, enzymatic biosensors usually showed unsatisfied sensitivity particularly in the detection of target substance at a relatively lower concentration. Thus, exploration of new detection mechanisms to simultaneously enhance the sensitivity and recognition capability of enzymatic biosensors is still on great demands (Chen et al., 2017; Wang et al., 2010).

Bi-enzymatic catalytic system has proved to be an effective approach to improve the biosensors' performance (Leite et al., 2003; Lin et al., 2014; Van et al., 2010). Its unique and promising detection mechanism was based on the coordinated catalysis mechanism as follows: targeted analyte could be oxidized by enzyme **a**, then, the

* Corresponding author.
** Corresponding author at: College of Materials Science and Engineering, Institute for Graphene Applied Technology Innovation, Collaborative Innovation Centre for Marine Biomass Fibers, Materials and Textiles of Shandong Province, Qingdao University, Qingdao 266071, China.
E-mail addresses: yhxu@qdu.edu.cn (Y. Xu), jliu@qdu.edu.cn (J. Liu).
[1] Tao Chen and Yuanhong Xu contributed equally to this work.

https://doi.org/10.1016/j.bios.2018.10.030

Available online 17 October 2018

obtained oxide could be subsequently reduced and regained by enzyme **b** (Bauer et al., 1999; Leite et al., 2003; Van et al., 2010). So, the concentration of targeted molecules would be always constant in the whole detection process of the bi-enzymatic catalytic system. Compared with mono-enzymatic biosensors, this system could effectively increase the sensitivity and recognition capability of enzymes in a lower target analyte concentration (Campanella et al., 1999; Oliveira et al., 2014; Perez et al., 2001). Till now, only several combinations of enzymes were used to construct the bi-enzymatic catalytic systems (Campanella et al., 1999; Chouteau et al., 2005; Manesh et al., 2010; Oliveira et al., 2014; Wang et al., 2012). Reasonable applications and optimizations of these collocations to achieve the higher detection performance are still promising and in great demand. Besides, current platforms for immobilization of enzymes are usually based on polypyrrole-block copolymer (Gürsel et al., 2003; Sun et al., 2015), carbon nanotubes nanocomposite (Karajanagi et al., 2004; Zhang et al., 2004), poly(thionine) film (Dempsey et al., 2004), chitosan nanocomposite films (Shan et al., 2010), among which the conducting polymers are the preferred precursors owing to their good electrical conductivities and easier implementation. As a kind of prospective structures with large surface area, nanoparticles (NPs) have been extensively utilized in biosensors, nanoreactors and nanocatalysis, etc. (C Li et al., 2008; Liu et al., 2012; Westesen et al., 1997), however, they were difficult to be prepared by above polymers. Therefore, NPs formed by new conducting polymers could be expected to provide an ideal platform in the construction of bi-enzymatic catalytic system to further enhance the biosensors sensitivity.

Poly-dopamine (PDA) (Dreyer et al., 2013), a sort of environment-friendly biopolymer with excellent biocompatibility, conductivity and stability, has attracted enormous interest in various applications such as coating (Dreyer et al., 2013), batteries (Shi et al., 2013), sensors (Hwang et al., 2014) and biomedical science (Lynge et al., 2011) in recent years. Moreover, structures with various morphologies could be easily controlled via altering the reaction conditions (Chien et al., 2012; Fu et al., 2014; Jiang et al., 2011). Therefore, it could be anticipated that PDA NPs could be utilized as a kind of ideal precursor for the construction of enzymes immobilization platform. Nevertheless, instead of the conducting polymer alone, combinations of polymers with metal nanoparticles have been found with apparent advantages such as obviously increased surface area and greatly enhanced acceleration of the electron transfer between immobilized biological recognition element and electrode due to the synergic effect of these two components (Rajesh et al., 2009; Xu et al., 2010). AuNPs (Hu et al., 2007), as an excellent choice with good conductivity (Sivakumar and Gedanken, 2005), biocompatibility (Xu et al., 2006) stability and large surface area (Lv et al., 2012) which could generate synergy on catalytic activity, could be chosen for the construction of bi-nanospherical signal amplification system.

Herein, via the oxidation polymerization of dopamine catalyzed by laccase (Tan et al., 2010), the laccase-loaded PDA NPs were successfully prepared by embedding the enzymes in PDA NPs during the polymerization process. AuNPs were then prepared by reduction of chloroauric acid and simultaneously anchored on the surface of PDA NPs uniformly. Subsequently, sulfydryl-functionalized glucose dehydrogenases were immobilized on the AuNPs surface to afford the bi-enzymatic and bi-nanospherical PDA-laccase@Au-glucose dehydrogenase. Based on the constructed bi-enzymatic system, a sensing platform for norepinephrine detection was successfully prepared and showed prominent sensitivity and stability. Besides, the as-prepared PDA-laccase@Au-glucose dehydrogenase was further applied as the sensing probes for the detection of microRNA (miRNA), especially for single-nucleotide mismatched miRNA via specific recognition. The stepwise synthesis of PDA NPs and fabrication of the biosensors were systematically characterized by ^{1}H NMR spectra, transmission electron microscope (TEM), X-ray diffraction (XRD), scanning electron microscope (SEM), and electrochemical measurements etc.

2. Experimental

2.1. Reagents and materials

Dopamine hydrochloride (AR), tris(hydroxymethyl)aminomethane hydrochloride (tris-HCl, AR), and ethylenediaminetetraacetic acid (EDTA, AR) were bought from Macklin Biochemical Co., Ltd. (Shanghai, China). Potassium hexacyanoferrate (III) ($K_3Fe(CN)_6$, AR), 2,2′-azino-bis (3-ethylbenzthiazoline-6-sulfonate) (ABTS, AR), potassium chloride (KCl, AR), potassium hexacyanoferrate (II) ($K_4[Fe(CN)_6]$, AR), sodium chloride (NaCl, AR) were bought from TCI Co. Ltd. (Shanghai, China). Dipotassium hydrogen phosphate trihydrate ($K_2HPO_4{\cdot}3H_2O$, AR), acetic acid (CH_3COOH, AR), sodium acetate (CH_3COONa, AR), n-hydroxysuccinimide (NHS, AR), 1-ethyl-3-(3-dimethyl-aminopropyl) carbodiimide hydrochloride (EDC, AR), ammonium hydroxide ($NH_3{\cdot}H_2O$, AR), potassium phosphate monobasic (KH_2PO_4, AR) were obtained from Tianjin Guangfu Co. Ltd. (Tianjin, China). Nafion (20 wt%) were purchased from Sigma–Aldrich Chemical Co. (Milwaukee, WI). Highly oriented pyrolytic graphite electrode, (HOPG, a kind of graphite working electrodes), Ag/AgCl reference electrodes and platinum foil auxiliary were purchased from Tianjin Aida Hengsheng Technology Co. Ltd. (Tianjin, China). *Fungal laccase* (*E.C. 1.10.3.2,* 0.5 U/mg solid) produced from the white-rot basidiomycete fungus Trametes (Coriolus, Polyporus) versicolor and *glucose dehydrogenase (EC 1.1.1.47)* were purchased from Shanghai Yuanye Bio-Technology Co. Ltd. (Shanghai, China). The laccase stock solution (1.0 mg/mL) was prepared using 0.1 M acetic acid buffer solution (ABS, pH 5.0) prior to usage. The norepinephrine solution (0.1 M) was freshly prepared in 0.1 M ABS (pH 5.0) prior to usage. The norepinephrine solutions at different concentrations used in the experiment were prepared by dilution of the norepinephrine solutions (0.1 M). Ultrapure water was obtained from the Flom ultrapure water system (Qingdao, China). PBS: 137 mM NaCl, 1.5 mM, KH_2PO_4, 8.1 mM Na_2HPO_4, 2.7 mM KCl, pH 7.4. Binding buffer: 200 mM Tris-HCl (pH 7.0), 1 M NaCl, 10 mM EDTA, 0.2% (v/v). The miRNA with certain sequences used in the experiments were custom-made from Sangon Biotech. (Shanghai, China).

2.2. Apparatus

Infrared spectra were measured on a Perkin-Elmer Spectrum One Fourier transform infrared (FTIR) spectra, equipped with the ATR accessory. The hydrodynamic diameter and size distributions of the obtained relevant particles were measured with dynamic light scattering (DLS, Zetasizer Nano ZS, Malvern Instruments). ^{1}H NMR spectra were measured on a JNM-ECP 600 (600 MHz) spectrometer. The molecular weight (Mw) distribution of laccase and laccase loaded PAD PNs were monitored by sodium dodecyl sulfate polyacrylamide gel electrophoresis (SDS-PAGE). Energy dispersive analysis (EDS) spectra were obtained from an EDS detector attached to the SEM microscope. Ultraviolet spectrophotometer (UV) spectra were measured on a UV/V-16/18 UV spectrophotometer (Shanghai, Mapada). The cyclic voltammetry (CV) assays were carried out on a CHI-760D electrochemical workstation (Shanghai, China). TEM images were obtained on JEOL 2010 TEM equipped with a LaB6 (lanthanum hexaboride) filament, operated at 200 KeV with GIF 2001 spectrometer and 1 megapixel CCD camera.

2.3. Synthesis of laccase-loaded PDA NPs

Laccase (0.05 g) was added to the dopamine solution (0.76 g, 2.15 mmol) in the mixture of water and ethanol (v/v = 1:1) as shown in Fig. 1A. The resulting mixed solution was stirred for 12 h at 4 °C. Then, the product was obtained via centrifugation for 20 min at 8000 rpm at 4 °C and washed with ice water for three times. The product (PDA-laccase) obtained after freeze drying were stored in refrigerator at 4 °C.

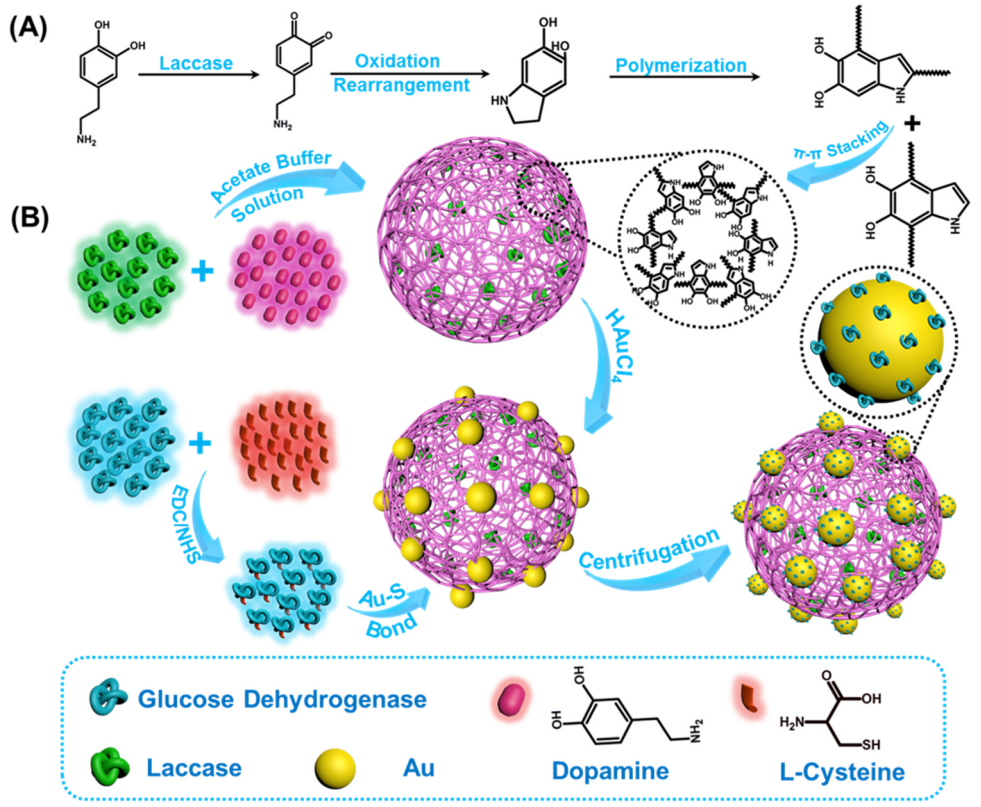

Fig. 1. The schematic illustration for the stepwise synthesis of (A) PDA NPs and (B) PDA-laccase@Au-glucose dehydrogenase.

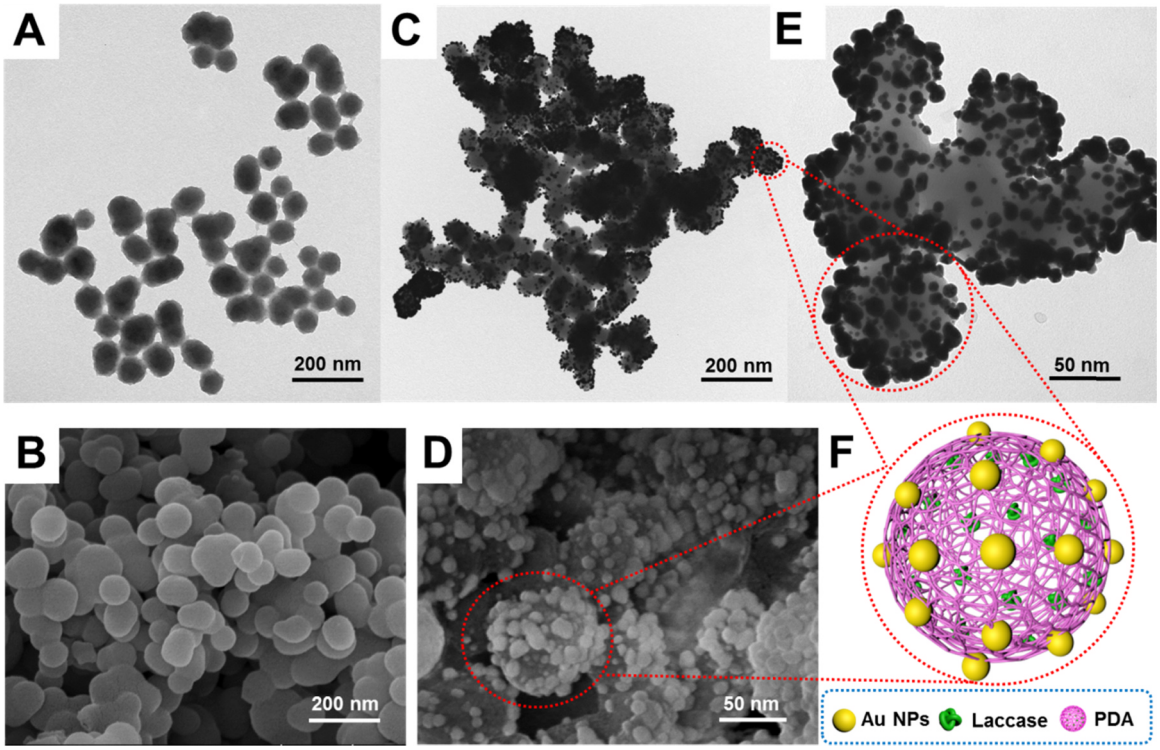

Fig. 2. The TEM (A) and SEM images (B) of the as-prepared PDA-laccase. The TEM (C) and (D) SEM images of the obtained PDA-laccase@Au. The amplified images (E) and supposed structures of PDA-laccase@Au (F).

2.4. Immobilization of AuNPs on laccase-loaded PDA NPs

1 mL water solution of $HAuCl_4$ (0.05 g/L) was dropwise added into the stirring solution of PDA-laccase (0.05 mg/mL) in a flask at 4 °C. The obtained mixture was allowed to proceed for 12 h at 4 °C. Then, the product was obtained via centrifugation for 15 min at 8000 rpm at 4 °C and washed with water for three times to afford the expected product (PDA-laccase@Au) after freeze drying and then stored in refrigerator at

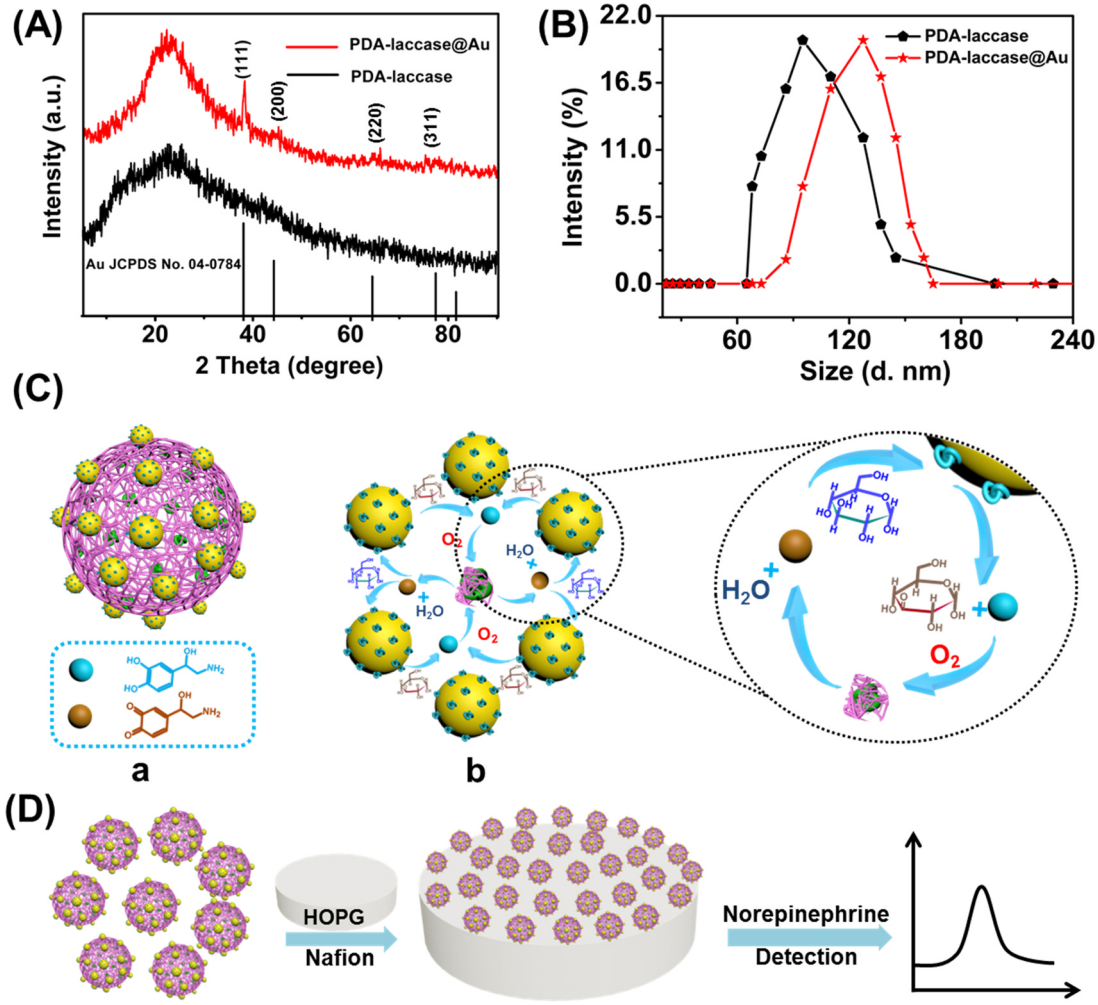

Fig. 3. (A) XRD spectra of PDA-laccase@Au and PDA-laccase. (B) DLS spectra of PDA-laccase and PDA-laccase@Au. (C) (a) The supposed micro-structure of PDA-laccase@Au-glucose dehydrogenase. (b) The supposed catalytic mechanism of the constructed platform based on bi-enzyme and bi-nanospheres. (D) Schematic illustration for facile fabrication of the biosensor for norepinephrine detection.

4 °C for usage after.

2.5. Synthesis of sulfydryl-functionalized glucose dehydrogenase (SH-glucose dehydrogenase)

2.5.1. Synthesis of NHS-functionalized glucose dehydrogenase

The synthesis of NHS-functionalized glucose dehydrogenase was carried out following the method we previously reported (Chen et al., 2017). Briefly, glucose dehydrogenase (60 mg) and EDC (48.0 mg, 0.25 mmol) were dissolved in ultrapure water (15 mL) in a 25 mL round-bottom flask. After stirring the mixture for 60 min, NHS (29.0 mg, 0.25 mmol) was added to the obtained mixed solution, and the resulting mixture was left stirring for 24 h at room temperature. Then, the obtained mixture was precipitated in cold diethyl ether for three times. The NHS-functionalized glucose dehydrogenase was obtained via centrifugation for 10 min at 12,000 rpm at 4 °C, washed with cold ultrapure water for three times and then stored in refrigerator at 4 °C after freeze drying for the following usage.

2.5.2. L-cysteine attachment to NHS-functionalized glucose dehydrogenase

Briefly, L-cysteine (5 mL of 50 mg/mL) of 0.1 M ABS (pH = 5.0) was dropwise added into NHS-functionalized glucose dehydrogenase solution (2 mL of 20 mg/mL) while stirring. The mixed solution was then incubated in ice-water bath with gentle shaking for 8 h. The free glucose dehydrogenase was cleared away through centrifugation at 12,000 rpm at 4 °C for 10 min, and washed with cold ultrapure water for three times, to obtain the pure sulfydryl-functionalized glucose dehydrogenase (Noted as SH-glucose dehydrogenase).

2.5.3. Attachment of SH-glucose dehydrogenase to PDA-laccase@Au

The way to combine –SH groups with AuNPs s were used in the method reported by Yi-Chun Wu et al. (Chen et al., 2006). The SH-glucose dehydrogenase sample (0.5 mg/mL, 3 mL) was added dropwise into the PDA-laccase@Au solution (1 mg/mL, 5 mL). The obtained solution was then kept shaking for 2 days in ice-bath. Then, the resulting mixed solution was centrifuged for 20 min at 5000 rpm and the supernatant was decanted to get rid of the unbound SH-glucose dehydrogenase. Finally, the obtained precipitate (PDA-laccase@Au-glucose dehydrogenase) was obtained and stored in refrigerator at 4 °C for the following usage (Fig. 1B).

2.6. Fabrication of the norepinephrine biosensor

Typically, 40 μL PDA-laccase@Au-glucose dehydrogenase solution (1 mg/mL) was dispersed in the same volume of 1.0 wt% Nafion solution by ultrasonication for 1 min to obtain a homogeneous, well-dispersed suspension of Nafion/PDA-laccase@Au-glucose dehydrogenase. The HOPG were modified by dripping the obtained Nafion/PDA-laccase@Au-glucose dehydrogenase on its surface, followed by evaporation of the solvents. The prepared electrodes were washed

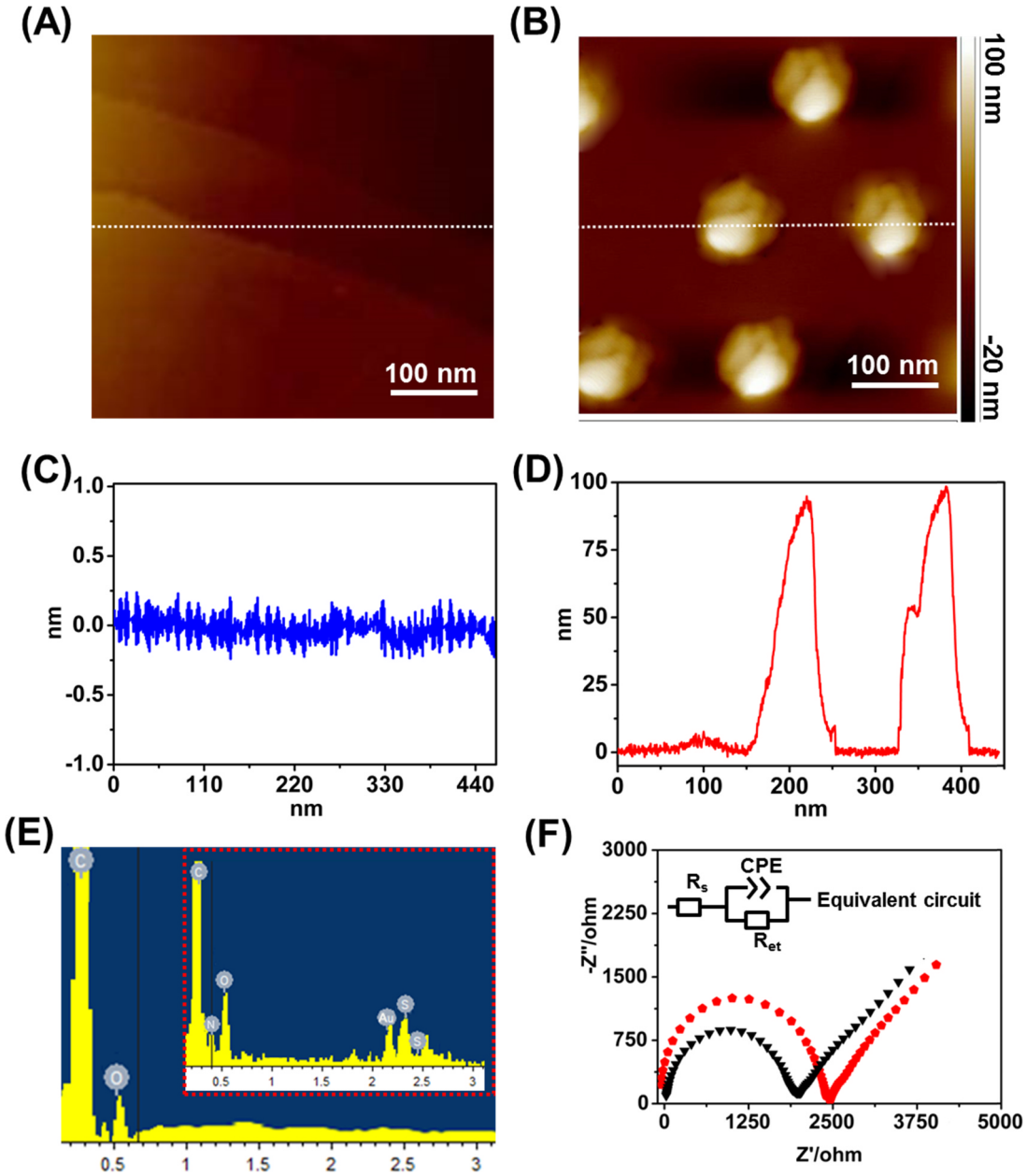

Fig. 4. AFM topography images (A, B) and corresponding height profiles (C, D) of bare (A, C) and (B, D) PDA-laccase@Au-glucose dehydrogenase modified HOPG surface. EDS spectra of (E) bare HOPG and PDA-laccase@Au-glucose dehydrogenase modified HOPG surface (insert). (F) Electrochemical impendence spectroscopy (ESI) measurement for (a) bare HOPG and (b) as-prepared biosensor in 5.0 mM $K_3[Fe(CN)_6]/K_4[Fe(CN)_6]$ (1:1) containing 50 mM KCl, respectively.

thoroughly using the deionized water to clear away the un-immobilized PDA-laccase@Au-glucose dehydrogenase and then stored in refrigerator at 4 °C for subsequent usages.

3. Results and discussion

3.1. Characterization of PDA-laccase and PDA-laccase@Au

Fig. 1A and B show the stepwise synthesis of PDA NPs and PDA-laccase@Au-glucose dehydrogenase. The successful preparation of PDA NPs was proved by ^{1}H NMR and FTIR spectra. As demonstrated in Fig. S1A, the obvious peak signals at 6.80–6.50 ppm should be assigned to the aromatic protons in dopamine while the peaks at 2.70 and 3.10 ppm are on behalf of the two methylene groups. As shown in the ^{1}H NMR spectrum of laccase in Fig. S1B, the peaks signals at 5.25 (f), 3.00 (g) are the main characteristic peaks of laccase. After polymerization of dopamine catalyzed by laccase, the ^{1}H NMR of the obtained polymers were tested and shown in Fig. S1C. It could be observed that the peak signals (6.80–6.50 ppm) of aromatic protons decreased compared to that of the monomer (dopamine), proving the successfully preparation of PDA. Moreover, compared to the ^{1}H NMR spectrum of PDA prepared via the traditional method (Fig. S1D), the characteristic peak signals of laccase (f and g) were observed in the spectrum of PDA-laccase prepared by the catalysis of laccase, confirming the successful immobilization of laccase on PDA NPs. As a control, laccase and PDA-laccase were also analyzed by FTIR and the results are shown in Fig. S2A. It can be seen from Fig. S2A(a), the characteristic peak signals in FTIR spectrum of laccase at 2910 cm^{-1} could be found in the spectrum of as-prepared PDA-laccase (Fig. S2A(b)), which further confirmed the presence of laccase in the as-prepared PDA-laccase. The successful preparation of PDA-laccase was further confirmed by SDS−PAGE analysis. As shown in Fig. S2B(a), the same stripe observed with the

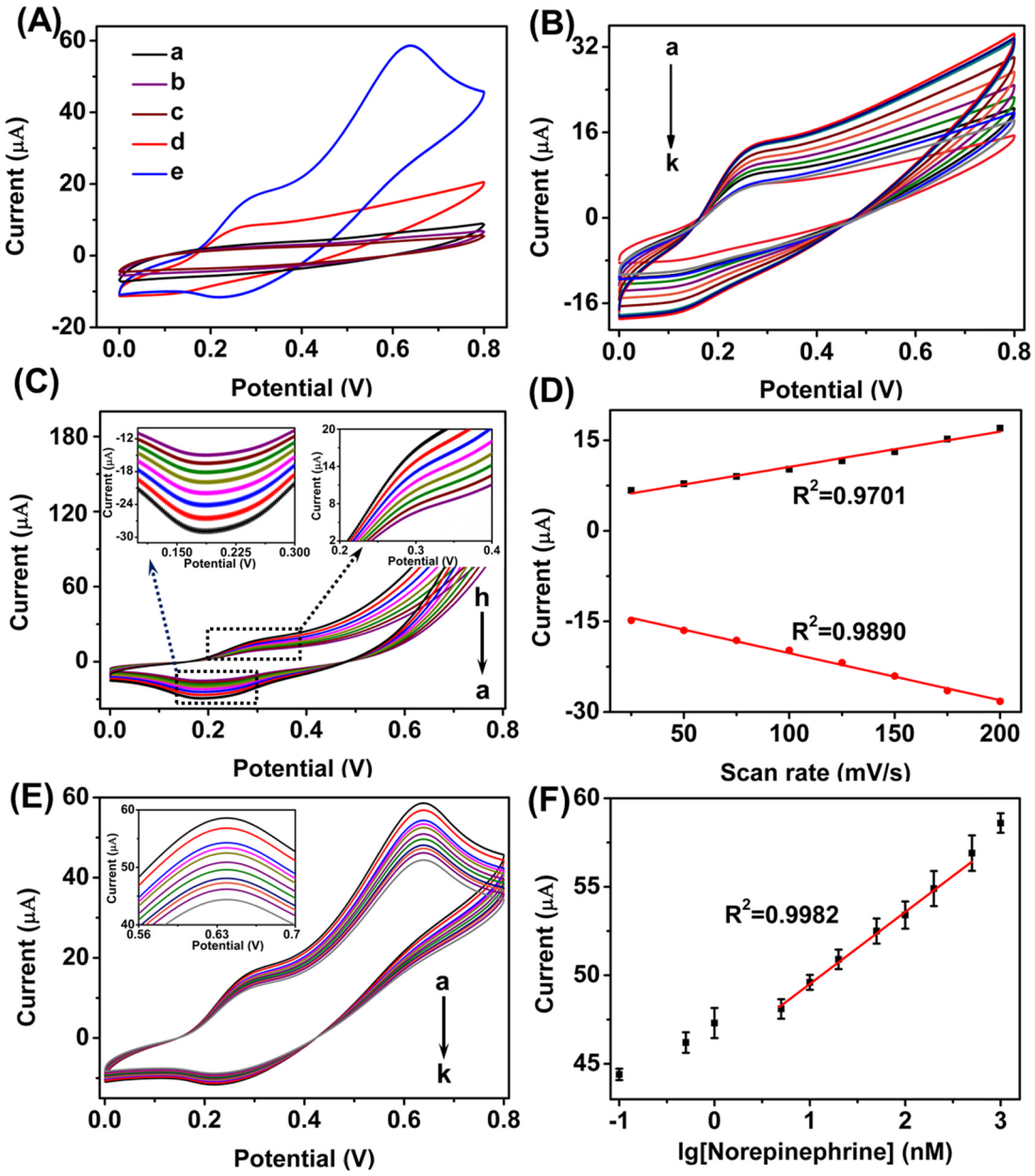

Fig. 5. (A) CV assays for the (a) bare HOPG, (b) PDA modified HOPG, (c) PDA@Au modified HOPG (d) PDA-laccase@Au-glucose dehydrogenase modified HOPG in 0.1 M ABS (pH 5.0) containing 5 mM glucose, (e) PDA-laccase@Au-glucose dehydrogenase modified HOPG in 0.1 M ABS (pH 5.0) containing 5 mM glucose and 5 mM norepinephrine. (B) The CVs assays for glucose in 0.1 M ABS (pH 5.0), at different concentrations. a, 5 mM; b, 1 mM; c, 0.5 mM; d, 0.1 mM; e, 50 μM; f, 10 μM; g, 5 μM; h, 1 μM; i, 0.5 μM; j, 0.1 μM, k, 50 nM. (C) CV assays for constructed biosensor at different scan rates: a, 25 mV/s; (b), 50 mV/s; (c), 75 mV/s; (d), 100 mV/s; (e), 125 mV/s; (f), 150 mV/s; (g), 175 mV/s and (h), 200 mV/s in 0.1 M ABS. (D) The anodic and cathodic peak currents against the scan rates. (E) The CVs assays using the as-prepared biosensor for norepinephrine with different concentrations of a, 1 μM; b, 0.5 μM; c, 0.1 μM; d, 50 nM; e, 10 nM; f, 5 nM; g, 1 nM; h, 0.5 nM; i, 0.1 nM; g, 0.05 nM; k, 0.01 nM in 0.1 M ABS (pH 5.0) containing 0.5 mM glucose. (F) The relationship between the logarithm of the norepinephrine concentration and corresponding CV current.

native laccase was found in the SDS-PAGE images of the obtained PDA-laccase while the new stripe observed with the SDS-PAGE image evidenced the larger Mw of PDA-laccase compared with that of native laccase, indicating that the laccase has been immobilized on the PDA NPs. Then, the bioactivity of the immobilized laccase was assessed in ABTS solution as shown in Fig. S2C. ABTS in the solution will be oxidized by laccase and the color will be changed into green (Chen et al., 2017). In the bioactivity test, the same amount of PDA prepared by the ammonium hydroxide oxidation and laccase oxidation were added to the ABTS solutions (1 mg/mL), respectively. It could be clearly observed that the color of ABTS solution changed from brown to dark green (left vessel in Fig. S2C) when PDA-laccase was added, while the color of solution in the absence of laccase (right vessel in Fig. S2C) almost unchanged. It proves that the pure PDA NPs cannot oxidize ABTS, laccase has been successfully immobilized on the as-prepared PDA, and the immobilized laccase still retained catalytical activity.

The SEM images (Fig. 2A) show that the as-prepared PDA NPs were spherical and about 100 nm in size, which was also proved by the TEM results as indicated in Fig. 2B. The AuNPs were generated by reduction of chloroauric acid and simultaneously fixed on the PDA NPs surface to obtain PDA-laccase@Au NPs which were also analyzed by SEM and TEM, respectively. Fig. 2C shows the presence of AuNPs on the PDA NPs surface, while the TEM analysis indicated the diameters of loaded AuNPs on PDA-laccase@Au was about 10 nm as shown in Fig. 2E. The

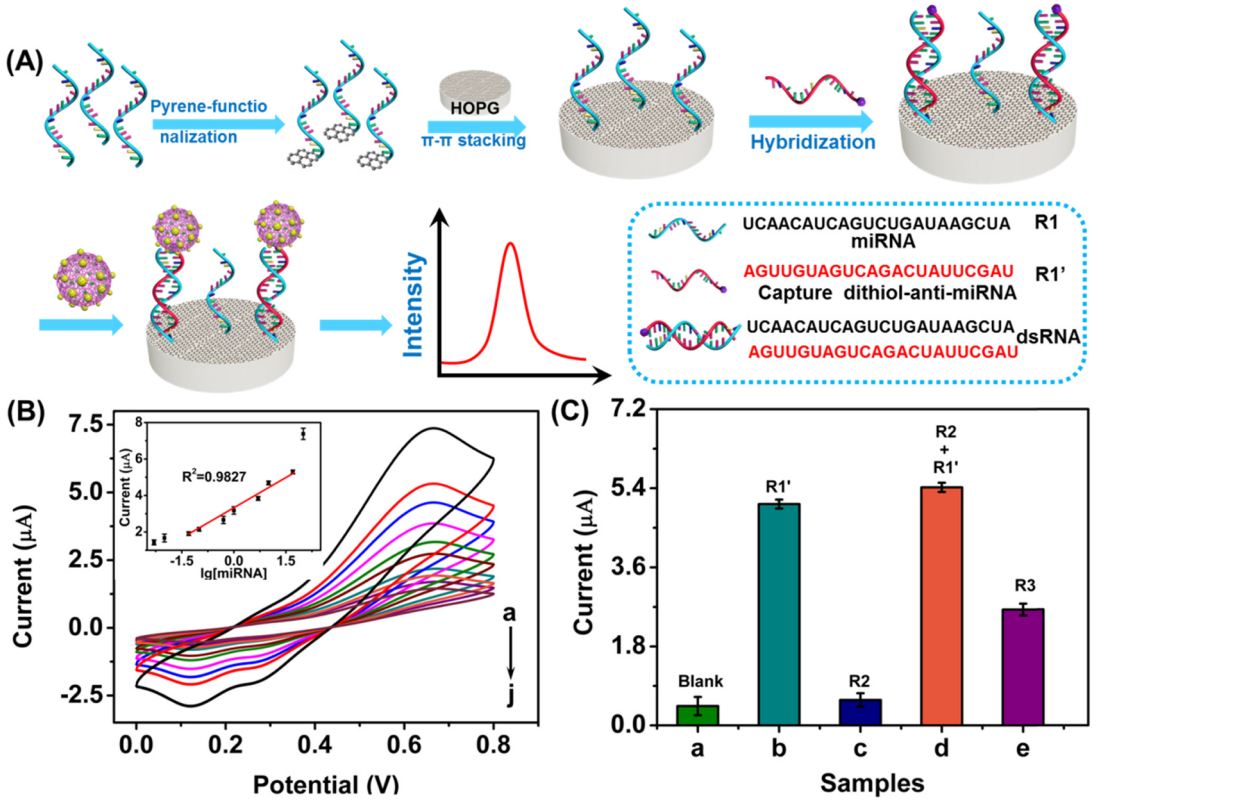

Fig. 6. Schematic of the preparation process of RNA (R1) modified HOPG and the specific recognition of the capture RNA (R1′). (B) The CVs assays in different concentrations of R1′ in PBS (pH 7.4) containing 0.5 mM glucose and 0.5 μM norepinephrine. a, 100 nM; b, 50 nM; c, 10 nM; d, 5 nM; e, 1 nM; f, 0.5 nM; g, 0.1 nM; h, 50 pM; i, 10 pM; j, 5 pM The insert is the relationship between the logarithm of the R1′ concentration and corresponding CV current. (C) Specificity investigation of the as-prepared sensing system for different nucleotide sequences. (a) Blank (PBS in the absence of the R1′), (b) R1′ (50 nM), (c) R2 (50 nM), (d) mixture of R1′ (50 nM) and R2 (50 nM), (e) R3 (50 nM), in PBS containing 0.5 mM glucose and 0.5 μM norepinephrine.

Table 1
All miRNA sequences used in this work.

Name of miRNA	Sequence
R1	5′-UCAACAUCAGUCUGAUAAGCUA-3′
R1	3′-AGUUGUAGUCAGACUAUUCGAU-5′-Sulfydryl
R2	3′-CGAUGUGGUGCGGCUGUUUGGU-5′-Sulfydryl
R3	3′-AGUUGUAGUCACACUAUUCGAU-5′-Sulfydryl

structure of the constructed PDA-laccase@Au could be clearly illustrated in Fig. 2F.

The XRD patterns were also obtained to reveal the structures of PDA-laccase and PDA-laccase@Au and the results are exhibited in Fig. 3A. As can be seen in Fig. 3A(a), a typical “bread” peak of PDA was observed, which proved that PDA was successfully prepared (Meng et al., 2017). The peaks at 2θ = 38.4°, 44.5°, 64.8° and 77.7° in the XRD pattern of PDA-laccase@Au (Fig. 3A(b)) should correspond to (111), (200), (220), and (311) planes of AuNPs in cubic crystal, which are in good agreement with JCPDS Card no. 04–0784 (Rao et al., 2017). These results confirmed that AuNPs were successfully prepared and anchored on the surface of PDA. The sizes of the obtained PDA and PDA-laccase@Au were analyzed by DLS and the results are shown in Fig. 3B. It can be found that the average diameter of PDA-laccase@Au was about 130 nm which was obviously larger than that of PDA (100 nm) due to the surface loading of AuNPs.

3.2. The supposed catalytic mechanism for the constructed bi-enzymatic platform

After the attachment of glucose dehydrogenase to PDA-laccase@Au via the Au-S bonds, the analytical platform based on bi-enzymes and bi-nanospheres (PDA-laccase@Au-glucose dehydrogenase were successfully constructed, as shown in Fig. 3C(a). The detailed catalytic mechanism for the bi-enzymes bioanalytical system is shown in Fig. 3C(b). It can be seen that the target analyte (norepinephrine) could be oxidized by laccase in the presence of oxygen, the obtained corresponding oxide could be subsequently reduced to be the primary target analyte (norepinephrine) by glucose dehydrogenase in the glucose solution. So, the norepinephrine concentration could remain constant in the whole detection process. Compared with the mono-enzymatic biosensors, this system could effectively increase the sensitivity and the signal stability in analysis of target analyte at a lower concentration. The biosensor was constructed by immobilization of PDA-laccase@Au-glucose dehydrogenase on HOPG using Nafion film as shown in Fig. 3D.

3.3. Fabrication and characterizations of the as-prepared biosensor

AFM images were collected to characterize the surface of bare and PDA-laccase@Au-glucose dehydrogenase modified HOPG. Fig. 4A revealed that the bare HOPG electrode surface was relatively flat (height ≤ 1 nm, Fig. 4C). However, obvious protuberances could be observed on the modified HOPG surface with the height about 100 nm (Fiugre 4B and 4D), proving the successful immobilization of PDA-laccase@Au-glucose dehydrogenase on HOPG surface. In addition, as shown in Fig. 4E, the EDS spectrum of the bare HOPG surface showed the presence of oxygen and carbon. However, after immobilization of PDA-laccase@Au-glucose dehydrogenase on HOPG, the elements of Au, S and the increased oxygen content were observed on the surface of electrode (insert of Fig. 4E). All of these characterizations above proved that the HOPG electrode was successfully modified. Besides, the EIS measurement for bare HOPG and the modified HOPG were also carried

out. As demonstrated in the insert of Fig. 4F, an equivalent circuit of the modified HOPG was applied for providing more information about the EIS. In the equivalent circuit, R_s refers to the electrolyte solution resistance while R_{et} represents the surface electron transfer resistance which reflects the surface conductivity of HOPG. As shown in Fig. 4F, the R_{et} for the bare HOPG electrode was 1780 Ω. Nevertheless, after the modification, the R_{et} of HOPG was enlarged to 2550 Ω. The obvious augment of the R_{et} further confirmed that the HOPG electrode surface was successfully modified with PDA-laccase@Au-glucose dehydrogenase.

3.4. Sensing performance of the as-prepared biosensor in norepinephrine detection

It could be seen from the curve a in Fig. 5A that no obvious peak was observed for the bare HOPG electrode. Moreover, no obvious peaks could be observed for both PDA modified and PDA@Au modified HOPG (curve b and cure c), indicating that the PDA and gold did not show any oxidation peaks in the tested potential. However, an obvious anodic peak at 0.24 V which should be assigned to the glucose dehydrogenase oxidation peak could be observed (Souza et al., 2016), indicating the successful modification of HOPG by glucose dehydrogenase. Then, after the addition of norepinephrine to the tested solution, an apparent peak at 0.6 V which is very close to the typical oxidation peak (0.58 V) (Chen et al., 2017; Li et al., 2012) of phenolic compounds could be observed as indicated in curve b of Fig. 5A. All of these results above indicated that both glucose dehydrogenase and laccase had been successfully fixed on the HOPG surface and the bi-enzymatic biosensors were successfully prepared. As shown in Fig. 5B, the CVs of biosensor were collected in ABS (0.1 M, pH 5.0) with different glucose concentrations. It was found that the oxidation current intensity enhanced with the increasing glucose concentration and would not increase anymore when the glucose concentrations are over 0.5 mM. Therefore, ABS with the addition of 0.5 mM glucose was chosen as the electrolyte media in the following study. Then, the CVs at different scan rates of the as-prepared biosensor were recorded and shown in Fig. 5C. Obviously, a large redox wave with oxidation peak at about 0.30 V was observed, which should be assigned to the characteristic redox wave of laccase. Moreover, as shown in Fig. 5D, both the cathodic and anodic current intensities were in proportion to the scan rate from 25 to 200 mV/s (R^2 = 0.9890 and R^2 = 0.9701, respectively), indicating the electrochemical reaction of on the HOPG surface was a surface-controlled electrochemical process (Chen et al., 2017; Qiu et al., 2013). Cyclic voltammetry was also carried out to further assess the sensing properties of the constructed biosensor for norepinephrine. As exhibited in Fig. 5E, the CV behaviors of the biosensor with different concentration of norepinephrine from 0.01 nM to 1 μM were measured. Fig. 5F shows good linearity in the concentration range of norepinephrine from 0.5 nM to 0.5 μM with R^2 = 0.9982. The detection limit was found to be as low as 0.07 nM (S/N = 3). The oxidation current intensity (I) was calculated by the following equation:

$$I = 45.3 + 4.22\lg[\text{norepinephrine}]$$

The sensitivity of the as-prepared biosensor is comparable or superior to those previously reported from other methods as shown in Table S1. As shown in Fig. S3A, no obvious redox behavior of norepinephrine at bare HOPG could be observed in the norepinephrine solution (0.5 nM), indicating the apparent signal amplification effect of the as-prepared biosensors (Limit of Detection = 0.07 nM). Moreover, the repeatability of the as-prepared biosensors were also tested using the same electrode and multi-electrodes. As shown in Fig. S3B, the peak current of the PDA-laccase@Au-glucose dehydrogenase modified electrode showed a slight decrease (8.57%) in a four-week frequent test, indicating its satisfied repeatability and stability. Besides, Fig. S3C indicated that the biosensors fabricated using the multi-electrodes also showed satisfied stability and repeatability.

3.5. Application of the bi-enzymatic signal amplification system in detection of miRNA

MiRNAs have been widely used as an important serum biomarker for clinical diagnose (Wei et al., 2017). However, the sensitive detection of miRNA is still a great challenge due to the interference of the large amount of miRNA with similar structures (Ambros et al., 2003; Carrington and Ambros, 2003). In our study, miRNA-21 (miRNA containing 21 nucleotides) was chosen as a model miRNA target because its wide distribution in cancerous organs such as brain, breast, colon, lung, ovary, liver, et al. (Naito et al., 2011; Pfeffer et al., 2015). The as-prepared PDA-laccase@Au glucose dehydrogenase was used as the sensing probes in the detection of miRNA-21 as shown in Fig. 6A. In detail, the pyrene-functionalized RNAs (R1) were immobilized on the surface of HOPG via π-π stacking between HOPG and the pyrene functionalized R1. As shown in Fig. S4, the emission fluorescence of pyrene functionalized R1 was mostly quenched after being immobilized onto graphene, which confirmed that R1 could be attached on HOPG surface via π-π stacking interaction between pyrene groups and graphene (Chen et al., 2018, 2017). Then, the modified HOPG was incubated in the R1′ solution for hybridization. After hybridization with R1′, the modified HOPG was then immersed in the PDA-laccase@Au glucose dehydrogenase (0.5 mg/mL) for the signal readout. Due to the Au-S bonds formed between the sulfydryl group of R1′ and AuNPs, the PDA-laccase@Au glucose dehydrogenase could be firmly immobilized on the HOPG surface. Therefore, the oxidization peak signals of the bi-enzymatic platform could be obtained. In order to obtain the optimized detection conditions, different sensing parameters were tested including incubation time used for miRNA hybridization, the PDA-laccase@Au glucose dehydrogenase concentration needed, and incubation time for signal readout. As shown in Fig. S5, 30 min for miRNA hybridization was enough for the modified HOPG to obtain the satisfied current signals. Then, different incubation time of the modified HOPG in the PDA-laccase@Au glucose dehydrogenase solution were tested. As shown in Fig. S6, the current signal intensity increased apparently with the prolongation of incubation time in 60 min. Therefore, 60 min for incubation was a proper time to achieve strong enough current signal. To decrease background signal and obtain better current intensity, the required concentration of PDA-laccase@Au glucose dehydrogenase in the assay system was also measured (Fig. S7). Accordingly, the concentration of PDA-laccase@Au glucose dehydrogenase was set at 5 mg/mL for the following sensing assays.

3.6. Sensing performance and interference study

After optimization, CVs against different R1′ concentrations were measured as shown in Fig. 6B. It could be observed that the oxidation peak current values enhanced with the enhanced concentration of R1′ from 5 pM to 100 nM. Accordingly, a wide detection range from 50 pM to 50 nM was obtained with a detection limit of 4 pM (S/N = 3) (Fig. 6B). The oxidation current intensity (I) was calculated by the following equation:

$$I = 3.301 + 1.148\lg[\text{R1}']$$

In order to study the selectivity of the as-prepared biosensor, a variety of different miRNAs were tested as the capture probe. As shown in Fig. 6C, obviously enhanced current intensity could be observed in the presence of R1′ (column b) compared to that in the absence of R1′ (column a). Besides, the signal of the biosensor in R2 solution (column c) is almost the same as that in the blank solution, and column d showed that the presence of R2 in R1 solution only resulted in a trivial effect on the obtained signals. All of the above results indicate that the higher signals result from the specific hybridization between R1 and target RNA, and R2 cannot hybridize with capture probe. Some diseases have been found to associate with gene mutation, most of which caused by a single-nucleotide mismatch (Fang et al., 2018). Thus, the sensors which

could efficiently distinguish the single-nucleotide mismatch is urgently needed in disease diagnosis. Thus, the single-nucleotide mismatch detection was also carried out. Accordingly, the biosensor was also utilized to test the R3 solution (single-nucleotide mismatched RNA, the detailed sequences of R3 is shown in Table 1, column e). Impressively, it was observed that the current obtained with the R3 solution was lower than that in R1′, confirming the discrimination capacity of the established biosensor in the analysis of single-nucleotide mismatched RNA. The ability of the biosensor to detect the single-nucleotide mismatched RNA is because the discontinuous mismatched double-stranded RNA (dsRNA) could inhibit the electron transfer between the sensing probes and electrode compared to that of well-matched RNA (Xiao et al., 2009). Besides, Figs. S8A and S8B indicated that the biosensors fabricated using the same electrode and multi-electrodes all showed satisfied stability and repeatability.

4. Conclusions

In summary, we have successfully constructed a bi-enzymatic and bi-nanospherical signal amplification system based on the designed PDA-laccase@Au-glucose dehydrogenase. The bi-nanospheres with large surface area and good conductivity provide a powerful platform for the firm immobilization of bi-enzymes, achieving the simultaneously enhanced sensitivity and stability of the as-prepared biosensor. Impressively, the biosensors based on this system showed good reproducibility, larger linear range of 0.5 nM–0.5 μM and a lower detection limit of 0.07 nM (S/N = 3) in the detection of norepinephrine. Besides, further applications of the proposed platform in specific recognition of miRNA was also proved to be satisfied, especially for the detection of single-nucleotide mismatched RNA distinction at a low concentration. It could be expected that the designed platform could envision promising clinical and biomedical applications, especially in mismatched RNA detection for genetic diagnosis in the future.

Acknowledgements

This work was supported by the National Natural Science Foundation of China (Nos. 21305133 and 21575071), Qingdao Innovation Leading Expert Program, Qingdao Basic & Applied Research Project (15-9-1–100-jch), Open Funds of the State Key Laboratory of Electroanalytical Chemistry (SKLEAC201601) and Science & Technology Fund Planning Project of Shandong Colleges and Universities (J16LA13).

Appendix A. Supporting information

Supplementary data associated with this article can be found in the online version at doi:10.1016/j.bios.2018.10.030.

References

Ambros, V., Bartel, B., Bartel, D.P., Burge, C.B., Carrington, J.C., Chen, X., Dreyfuss, G., Eddy, S.R., Griffiths-Jones, S., Marshall, M., 2003. RNA 9 (3), 277–279.
Bauer, C.G., Kühn, A., Gajovic, N., Skorobogatko, O., Holt, P.-J., Bruce, N.C., Makower, A., Lowe, C.R., Scheller, F.W., 1999. Fresen. J. Anal. Chem. 364 (1–2), 179–183.
C Li, Y.L., Li, L., Du, Z., Xu, S., Zhang, M., Yin, X., Wang, T., 2008. Talanta 77 (1), 455–459.
Campanella, L., Favero, G., Sammartino, M.P., Tomassetti, M., 1999. Anal. Chim. Acta 393 (1–3), 109–120.
Carrington, J.C., Ambros, V., 2003. Science 301 (5631), 336–338.
Chao, W., Liu, X., Li, Y., Du, X., Xia, W., Ping, X., 2014. Biosens. Bioelectron. 53 (6), 26–30.
Chen, C.C., Lin, Y.P., Wang, C.W., Tzeng, H.C., Wu, C.H., Chen, Y.C., Chen, C.P., Chen, L.C., Wu, Y.C., 2006. J. Am. Chem. Soc. 128 (11), 3709–3715.
Chen, T., Li, M., Liu, J., 2018. Cryst. Growth Des. 18 (5), 2765–2783.
Chen, T., Xu, Y., Peng, Z., Li, A., Liu, J., 2017. Anal. Chem. 89 (3), 2065–2072.
Chen, Z., Liu, Y., Wang, Y., Zhao, X., Li, J., 2013. Anal. Chem. 85 (9), 4431–4438.
Chien, H.W., Kuo, W.H., Wang, M.J., Tsai, S.W., Tsai, W.B., 2012. Langmuir 28 (13), 5775–5782.
Chouteau, C., Dzyadevych, S., Durrieu, C., Chovelon, J.M., 2005. Biosens. Bioelectron. 21 (2), 273–281.
Dempsey, E., Diamond, D., Collier, A., 2004. Biosens. Bioelectron. 20 (2), 367–377.
Dreyer, D.R., Miller, D.J., Freeman, B.D., Paul, D.R., Bielawski, C.W., 2013. Chem. Sci. 4 (10), 3796–3802.
Fang, Y., Yang, X., Chen, T., Xu, G., Liu, M., Liu, J., Xu, Y., 2018. Sens. Actuators B 263, 400–407.
Fu, Y., Liu, L., Zhang, L., Wang, W., 2014. ACS Appl. Mater. Interfaces 6 (7), 5105–5112.
Gürsel, A., Alkan, S., Toppare, L., Yağcı, Y., 2003. React. Funct. Polym. 57 (1), 57–65.
He, Y., Li, J., Liu, Y., 2015. Anal. Chem. 87 (19), 9777–9785.
Hu, J., Wang, Z., Li, J., 2007. Sensors 7 (12), 3299–3311.
Hwang, S.H., Kang, D., Ruoff, R.S., Shin, H.S., Park, Y.B., 2014. ACS Nano 8 (7), 6739–6747.
Jiang, J., Zhu, L., Zhu, B., Xu, Y., 2011. Langmuir 27 (23), 14180–14187.
Karajanagi, Sandeep S., Vertegel, Alexey A., Kane, Ravi S., Dordick, Jonathan S., 2004. Langmuir 20 (26), 11594–11599.
Kwok, R.T., Leung, C.W., Lam, J.W., Tang, B.Z., 2015. Chem. Soc. Rev. 44 (13), 4228–4238.
Lanzellotto, C., Favero, G., Antonelli, M.L., Tortolini, C., Cannistraro, S., Coppari, E., Mazzei, F., 2014. Biosens. Bioelectron. 55 (55), 430–437.
Leite, O.D., Lupetti, K.O., Fatibello-Filho, O., Vieira, I.C., Barbosa, A.M., 2003. Talanta 59 (5), 889–896.
Li, J., Cheng, G., Dong, S., 1996. J. Electroanal. Chem. 416 (1–2), 97–104.
Li, Y., Qin, C., Chen, C., Fu, Y., Ma, M., Xie, Q., 2012. Sens. Actuators B 168, 46–53.
Lin, L., Yan, J., Li, J., 2014. Anal. Chem. 86 (21), 10546–10551.
Liu, J., Qiao, S.Z., Chen, J.S., Lou, X.W., Xing, X., Lu, G.Q., 2012. ChemInform 43 (6), 12578–12591.
Lu, X., Wen, Z., Li, J., 2006. Biomaterials 27 (33), 5740–5747.
Lv, Y., Lin, Z., Svec, F., 2012. Anal. Chem. 84 (20), 8457–8460.
Lynge, M.E., Van, dW.R., Postma, A., Städler, B., 2011. Nanoscale 3 (12), 4916–4928.
Manesh, K.M., Santhosh, P., Uthayakumar, S., Gopalan, A.I., Lee, K.P., 2010. Biosens. Bioelectron. 25 (7), 1579–1586.
Meng, R., Chen, Y., Zhang, X., Dong, X., Ma, H., Wang, G., 2017. J. Macromol. Sci. A 54 (5), 334–338.
Naito, M., Katayama, R., Ishioka, T., Suga, A., Takubo, K., Nanjo, M., Hashimoto, C., Taira, M., Takada, S., Takada, R., 2011. RNA Biol. 8 (5), 706–713.
Oliveira, T.M., Barroso, M.F., Morais, S., Araújo, M., Freire, C., De, L.-N.P., Correia, A.N., Oliveira, M.B., Delerue-Matos, C., 2014. Bioelectrochemistry 98 (2), 20–29.
Perez, E.F., Neto, G.D.O., Kubota, L.T., 2001. Sens. Actuators B 72 (1), 80–85.
Pfeffer, S.R., Yang, C.H., Pfeffer, L.M., 2015. Drug Dev. Res. 76 (6), 270–277.
Qiao, H., Soeriyadi, A.H., Guan, B., Reece, P.J., Gooding, J.J., 2015. Sens. Actuators B 211, 469–475.
Qiu, L.P., Qiu, L., Wu, Z.S., Shen, G.L., Yu, R.Q., 2013. Anal. Chem. 85 (17), 8225–8231.
Rajesh, Ahuja, T., Kumar, D., 2009. Sens. Actuators B 136 (1), 275–286.
Rao, H., Min, C., Ge, H., Lu, Z., Xin, L., Ping, Z., Wang, X., Hua, H., Zeng, X., Wang, Y., 2017. Biosens. Bioelectron. 87, 1029–1035.
Rasooly, A., Herold, K.E., 2006. J. AOAC Int. 89 (3), 873–883.
Sassolas, A., Blum, L.J., Leca-Bouvier, B.D., 2012. Biotechnol. Adv. 30 (3), 489–511.
Shan, C., Yang, H., Han, D., Zhang, Q., Ivaska, A., Niu, L., 2010. Biosens. Bioelectron. 25 (5), 1070–1074.
Shen, M.Y., Li, B.R., Li, Y.K., 2014. Biosens. Bioelectron. 60 (1), 101–111.
Shi, J.L., Fang, L.F., Li, H., Zhang, H., Zhu, B.K., Zhu, L.P., 2013. J. Membr. Sci. 437 (12), 160–168.
Sivakumar, M., Gedanken, A., 2005. Synth. Met. 148 (3), 301–306.
Song, Y., Luo, Y., Zhu, C., Li, H., Du, D., Lin, Y., 2016. Biosens. Bioelectron. 76, 195–212.
Souza, J.C.P.D., Iost, R.M., Crespilho, F.N., 2016. Biosens. Bioelectron. 77, 860–865.
Sun, C., Wang, D., Zhang, M., Ni, Y., Shen, X., Song, Y., Geng, Z., Xu, W., Liu, F., Mao, C., 2015. Analyst 140 (3), 797–802.
Tan, Y., Deng, W., Li, Y., Huang, Z., Meng, Y., Xie, Q., Ma, M., Yao, S., 2010. J. Phys. Chem. B 114 (15), 5016–5024.
Van, H.W., Ludwig, R., Dewulf, J., Auly, M., Messiaen, T., Haltrich, D., Van, L.H., 2010. Biotechnol. Bioeng. 102 (1), 122–131.
Wang, H., Yuan, R., Chai, Y., Niu, H., Cao, Y., Liu, H., 2012. Biosens. Bioelectron. 37 (1), 6–10.
Wang, H., Wang, X., Zhang, X., Qin, X., Zhao, Z., Miao, Z., Huang, N., Chen, Q., 2010. Biosens. Bioelectron. 25 (1), 142–146.
Wei, T., Du, D., Wang, Z., Zhang, W., Lin, Y., Dai, Z., 2017. Biosens. Bioelectron. 94, 56–62.
Westesen, K., Bunjes, H., Koch, M.H.J., 1997. J. Control. Release 48 (2), 223–236.
Wooten, M., Karra, S., Zhang, M., Gorski, W., 2014. Anal. Chem. 86 (1), 752–757.
Xiao, Y., Lou, X., Uzawa, T., Plakos, K.J.I., Plaxco, K.W., Soh, H.T., 2009. J. Am. Chem. Soc. 131 (42), 15311–15316.
Xu, J., Wang, K., Zu, S.Z., Han, B.H., Wei, Z., 2010. ACS Nano 4 (9), 5019–5026.
Xu, Q., Mao, C., Liu, N.N., Zhu, J.J., Sheng, J., 2006. Biosens. Bioelectron. 22 (5), 768–773.
Zhang, L., Zhang, Q., Lu, X., Li, J., 2008. Biosens. Bioelectron. 23 (1), 102–106.
Zhang, M., Smith, A., Gorski, W., 2004. Anal. Chem. 76 (17), 5045–5050.
Zhang, Q., Qiao, Y., Hao, F., Zhang, L., Wu, S., Li, Y., Li, J., Song, X.M., 2010. Chemistry 16 (27), 8133–8139.